[Article] www.whxb.pku.edu.cn

簇形和花形 CdS 纳米结构的自组装及光催化性能

许 迪 高爱梅 邓文礼*
(华南理工大学材料科学与工程学院, 广州 510640)

摘要: 通过可控溶剂热法, 利用乙二胺作为模板制备出簇形和花形硫化镉(CdS)纳米结构. 通过 X 射线衍射(XRD)和扫描电镜(SEM)观测其形貌和结构特征. XRD 谱线显示, 簇形 CdS 为六方晶体结构, 而花形 CdS 纳米结构则为立方晶体. 实验结果表明, 整个自组装过程是由成核以及成核竞争引起的不同生长过程所组成的, 并且乙二胺的模板功能起了重要的作用. 通过不同时间和温度的实验, 深入探讨了簇形和花形 CdS 纳米结构的自组装机理. 室温光致发光谱(PL)显示这两种纳米结构在 433 nm 和 565 nm 附近有较强的发射峰, 分别对应激子发射和表面缺陷发光. 通过 Brunauer-Emmett-Teller (BET)方法测试其比表面积. 研究了高压汞灯照射下, 簇形和花形 CdS 纳米结构在甲基橙(MeO)溶液中的光催化性能. 结果显示, 由于其较大的比表面积, 花形 CdS 纳米结构的光催化性能要远优于其它 CdS 材料.

关键词: 硫化镉; 纳米棒簇; 花形纳米结构; 自组装; 光催化
中图分类号: O649; O643

Self-Assembly and Photocatalytic Properties of Clustered and Flowerlike CdS Nanostructures

XU Di GAO Ai-Mei DENG Wen-Li*
(*College of Materials Science and Engineering, South China University of Technology, Guangzhou 510640, P. R. China*)

Abstract: Clustered and flowerlike CdS nanostructures were synthesized *via* the controllable solvent thermal method using ethylenediamine as the structure-directing template. The phase structures and morphologies were measured by X-ray diffraction (XRD) and scanning electron microscopy (SEM). XRD patterns demonstrated that the CdS nanorod cluster sample was hexagonal cell and the flowerlike CdS nanostructure was cubic cell. Experimental results showed that the whole self-assembly process was made-up of nucleation and growth, which was due to the competition in the nucleation. And the template function of ethylenediamine played an important role in the self-assembly. The self-assembly mechanisms of forming the clustered and flowerlike nanostructures were investigated on the basis of the time- and temperature-dependent experiments and were briefly discussed. At room temperature, photoluminescence (PL) spectrum experiments revealed that CdS nanostructures had two visible emission peaks respectively at the wavelengths of 433 nm and nearly 565 nm, which should arise respectively from the excitonic emission and surface-defect. The specific surface areas were characterized by the Brunauer-Emmett-Teller (BET) method. The photocatalysis of clustered and flowerlike CdS nanostructures in methyl orange (MeO) under high-pressure mercury lamp illumination was investigated. The experimental results indicated that the performance of photocatalytic system employing flowerlike CdS nanostructure, with higher specific surface area, was observed to be better than other CdS materials.

Key Words: CdS; Nanorod clusters; Flowerlike nanostructures; Self-assembly; Photocatalysis

Received: January 10, 2008; Revised: March 27, 2008; Published on Web: May 28, 2008.
*Corresponding author. Email: wldeng@scut.edu.cn; Tel: +8620-22236708.
国家自然科学基金(20643001)、广东省科技计划项目(20061311801002)和广州市重点科技攻关项目(2006Z3-D2021)资助

More and more material scientists are attempting to fabricate novel materials. Three-dimension (3D) nanostructures have attracted much attention because of their unique properties and potential applications[1–7]. Most 3D nanostructures are synthesized *via* self-assembly, that is, ordered aggregations are formed in a spontaneous process[2]. It is important to develop a simple and reliable synthetic process for hierarchically self-assembled architectures with designed chemical components and controlled morphologies. CdS nanostructures have been studied in diverse fields including photoelectric sensors[8], photocatalysis[9], luminescence[10], and laser driver[11]. Approaches to synthesize CdS nanostructures include catalyzed growth by the vapor-liquid-solid mechanism at a high temperature[12], the template-based synthesis by electrochemical fabrication[13] and the use of solvent thermal conditions or wet chemistry[14,15].

Although many kinds of flowerlike structures, such as CdS with $Cd_4Cl_3(OH)_5$ used as precursor[16], carbonated hydroxyapatite sphere[17], and metal oxides[18–20], have been reported, the controlling mechanism of forming CdS nanostructures remains inconclusive. The self-assembly of low-dimensional building blocks into complex 3D nanostructures is still considerably difficult and need to be explored in detail. This paper deals with the CdS nanorod clusters and flowerlike nanostructures synthesized directly by an ethylenediamine-mediated solvent thermal method. To explore the key factor in the formation of various nanostructures, we systematically chose different synthetic reaction times and temperatures. Scanning electron microscopy (SEM) and X-ray powder diffraction (XRD) were used to characterize the fancy CdS nanostructures. At room temperature, photoluminescence (PL) measurements were also carried out to further characterize the photophysical properties of the CdS nanostructures. The experimental results of photoluminescence confirmed that the synthesized CdS nanostructures were of a higher optical quality than the commercial CdS products. The formation mechanism and self-assembly process are discussed briefly based on the experimental data.

Methyl orange (MeO) is an azo dye and also has a variety of uses in textiles, pulp, paper and leather industry. The release of MeO and its products in the environment cause toxicity problems[21,22]. Many attempts have been made to study the decolorization of the dye. Since Fujishima and Honda[23] reported a TiO_2 photochemical electrode for splitting water in 1972, photocatalysis has drawn increasing attention. The general photocatalytic process of a semiconductor involves the formation of photoinduced electrons at the conduction band and holes at the valence band, and the subsequent chemical reactions with the surrounding media after photostimulated charges move to the surface. CdS is generally considered to be one of the effective photocatalysts and has the ability to detox water from a number of organic pollutants. Especially, the high surface area of flowerlike CdS nanostructure enhances photocatalytic activity as it provides an environment for high concentration of target organic substances around sites activated by ultraviolet radiation, and so the rate of photocatalysis is improved. In the present paper, the application for photocatalysis was carried out in MeO solution with different CdS catalysts. The experimental results of photoluminescence and photocatalysis confirmed that the synthesized flowerlike CdS nanostructure had higher specific surface area and photocatalytic property than the clustered CdS nanostructure and common commercial CdS product.

1 Experimental

1.1 Sample preparation

All the chemicals were analytically graded and used without further purification. CdS compounds were synthesized by the solvent-thermal method. $SC(NH_2)_2$ solution and $Cd(NO_3)_2 \cdot 4H_2O$ solution at a molar ratio of 1∶1 was added to a Teflon-lined stainless steel autoclave with a capacity of 100 mL. Then the autoclave was filled with 10% of ethylenediamine ($C_2H_8N_2$) solution, till about 80% of the total volume. The pellucid solution obtained was stirred with a magnetic stirrer and treated with ultrasonic. The autoclave was maintained at 353–443 K for 4–48 h and then allowed to cool to room temperature. Yellow and red precipitates were collected and washed with absolute ethanol and distilled water to remove residues of organic solvent. The final products were dried at 353 K for 4 h in a vacuum box.

1.2 SEM and XRD characterization

The samples were characterized by scanning electron microscopy (SEM, Philips FEI-XL30) operating at 25 kV and by X-ray powder diffraction (XRD, Panlytical XpertPRO diffractometer with Cu K_α radiation, λ=0.1542 nm, 40 kV, 40 mA).

1.3 Photoluminescence measurement

The photoluminescence (PL) experiments were performed on a Fluorolog-3 spectrofluorimeter (Jobin-Yvon Inc., Longjumeau, France) at room temperature. The contrastive CdS powder material used in the photoluminescence experiments was purchased from Chongqing Instrument Material Research Institute (pure grade > 99.999%, average diameter < 3 μm).

1.4 Photocatalysis measurement

The Brunauer-Emmett-Teller (BET) specific surface areas were determined through nitrogen adsorption at 473 K using a Micromeritics Flowsorb-3 2310 instrument.

The photocatalytic oxidation of methyl orange (MeO) in suspension of CdS under high-pressure mercury lamp illumination was studied, to test the photocatalytic activity of the nanorod clusters and flowerlike CdS nanostructures. 200 mL MeO solution (40 mg·L^{-1}) was employed as a target. The mixture inside a 500 mL beaker remained in suspension by using magnetic stirrers. A 250 W high-pressure mercury lamp (GYZ-250) fixed at a distance of 30 cm above the surface solution. The whole instrument was set in an occluded light box. The absorbance of the MeO solution was measured with a UV-visible spectrophotometer (Hitachi U-3010 UV-Vis spectrometer).

The absorption spectra were recorded and rate of decolorization was observed in terms of change in intensity at λ_{max} (nearly 462 nm) of the MeO. The decolorization efficiency (η) has been

calculated as:

$$\eta=(A_0-A)/A_0\times100\% \quad (1)$$

where A_0 is the initial concentration of MeO and A is the concentration of MeO after irradiation. The contrastive CdS powder material used was the same in the PL measurement.

2 Results and discussion

Ethylenediamine was used as a solvent, and CdS nanostructures were prepared *via* the solvothermal reaction of Cd^{2+} and S^{2-} at different temperatures for different times. The schematic process is shown as follows:

$$Cd^{2+}+C_2H_8N_2 \longrightarrow \left[\begin{array}{cc} H_2CH_2N & NH_2CH_2 \\ & Cd \\ H_2CH_2N & NH_2CH_2 \end{array}\right]^{2-} \quad (2)$$

(Cd-complex)

$$\text{Cd-complex}+SC(NH_2)_2 \longrightarrow CdS+C_2H_8N_2 \quad (3)$$

With the change of temperature and time, the reactions produced various nanostructures, such as particle chain balls (Fig. 1a), hexagonal nanorod clusters (Fig.1b), and flowerlike CdS nanostructures (Fig.1(c, d)). Experiments revealed that the entire flowerlike CdS nanostructures were built from dozens of petals with smooth surfaces. These petals were about 80 nm thick and 1 μm wide. Reaction time and temperature played crucial roles in controlling the nucleation and the growth of crystallites. We made full use of these obtained results to describe the chemical synthesis method and self-assembly process in the controlling of crystal shape, size, and structure.

Fig.2a shows a wide-angle XRD pattern of the CdS nanorod cluster sample, which can be described as the hexagonal of CdS (space group: *P*63*mc*(186), *a*=*b*=0.4132 nm, *c*=0.6734 nm; JCPDS card No. 65-3414). XRD experiments demonstrate the presence of crystalline CdS. The unusually strong (002) peak in the pattern indicates a preferential orientation of (001) in CdS nanorod[24]. However, in the XRD pattern (Fig.2b) of the flowerlike CdS nanostructure obtained from the final stage, all the reflections can be indexed to the cubic cell of CdS with lattice constant *a*=0.5832 nm equivalent to the values of JCPDS 65-2887, which is in agreement with the reported value[25]. The significant broadening of the diffraction peaks shown in Fig.2b indicates that the particle size of flowerlike nanostructure is smaller. And it also presents evidence of the higher specific surface area than others.

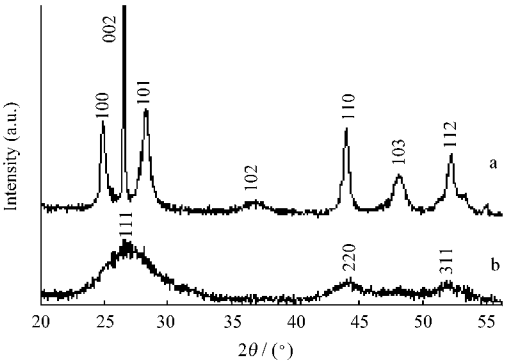

Fig.2 XRD patterns of obtained samples

(a) CdS nanorod cluster; (b) flowerlike CdS nanostructure

In order to understand the enormous structural difference between the two kinds of CdS nanostructures, we carried out a series of experiments at different temperatures for different times. According to the classical crystal growth theory of Buhro[26], the formation of nanostructure includes the both processes of nucleation and growth. At the initial nucleation, if the concentration of composed particles, such as atoms, ions, or molecules, is high enough, the particles are assembled into a small cluster. With the offered component particles and the working template function, the small cluster will grow into a crystal core. So, we study the first stage namely nucleation process without coordination agent.

Fig.3 shows SEM images of CdS cores obtained from the beginning stage, two different crystal core samples were collected at 423 K for 4 h without ethylenediamine. One is smooth micro

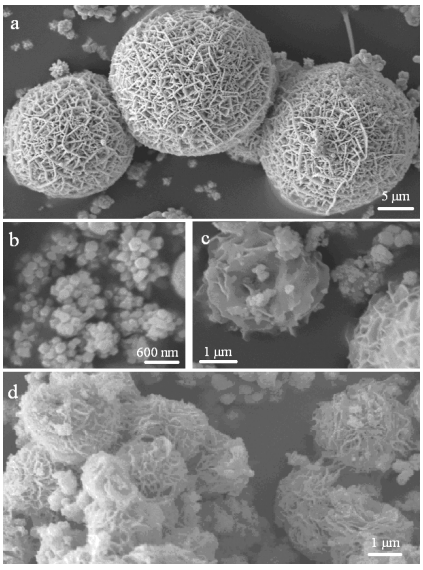

Fig.1 SEM images of CdS nanostructures

(a) CdS particle chain balls formed at 423 K for 8 h;
(b) CdS nanorod clusters formed at 423 K for 6 h;
(c, d): flowerlike CdS nanostructures formed at 423 K for 24 h

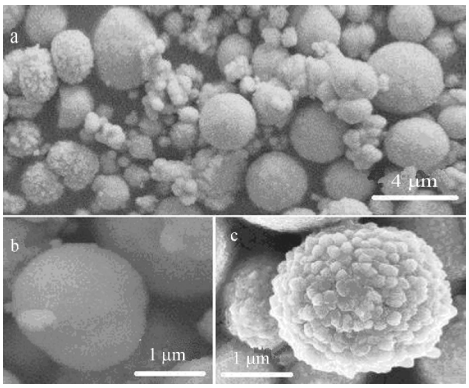

Fig.3 SEM images of CdS cores collected at 423 K for 4 h

(a) large area SEM image of smooth micro spheres and hexagonal single crystal balls; (b) smooth micro sphere; (c) hexagonal crystal ball

sphere with a diameter of about 3 μm (Fig.3b), and the other is reunite body comprised of hexagonal crystal with a diameter of about 2 μm (Fig.3c). As the reaction proceeded and the template function appeared, they began to grow along different routes. The whole evolution process is described in Fig.4. Under the ethylenediamine template, by embosoming the smooth micro spheres, the nanometer particles reunited tightly for 8 h and formed particle chains which enwrapped intensively the interior micro sphere, as shown in Fig.1a. To prolong time to 12 h, the particles composed of chains merged each other, and the discrete chain changed into the uninterrupted line gradually. As the line became thinner and wider 24 h later, the micro sphere grew into the flowerlike nanostructure. In the final stage, the flowerlike nanostructure was stably maintained, not changing anymore with time passing. In the experiments at different temperatures, we fortunately found that there existed a similar growth course. As temperature rose from 353 to 443 K, not only the quantity of the flowerlike nanostructure increased but also its perfect structure exhibited fully.

On the other hand, the hexagonal crystal ball also grew along the ethylenediamine template. Under the function of template, the crystal core grew into the hexagonal nanorod cluster. In the experiments at different temperatures, we found that the nanorod grew perfectly at the temperature over 373 K, the feature of which was that the nanorod grew up comparatively slowly. To prolong time, the nanorod was got thicker, longer, and more densely.

The possible pathway of 3D CdS nanostructure self-assembly was proposed. We think that the competition between reunion and growth of core is the first reason for forming different cores. If the reunion factor is dominant, the small crystal cores will aggregate into crystal balls under some surface physical and chemical effects, such as electrostatic and van der Waals forces. However, if the growth factor is dominant, Cd^{2+} and S^{2-} ions assemble on individual CdS particle constantly until it grows into a smooth micro sphere. To fully understand what reason effectively induces the development of competition which controls the way of self-assembly, more investigations are needed.

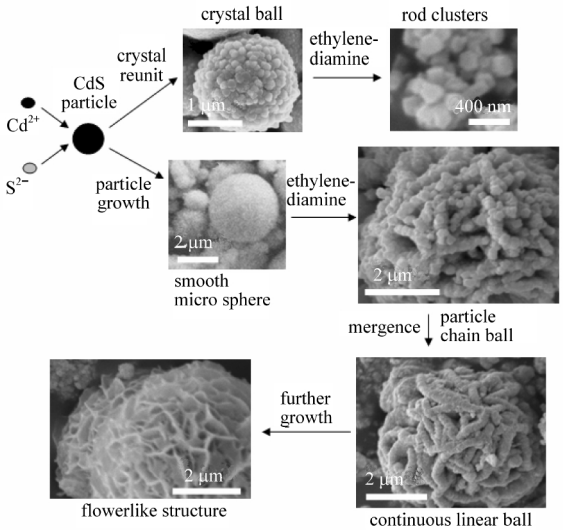

Fig.4 Schematic illustration of the morphological evolution process of CdS nanostructures

The ethylenediamine played an important role in the self-assembly of CdS nanostructures. In the solution, the solvent ethylenediamine molecule acted as a bidentate ligand to form relatively planar Cd-complex, which was favorable to Cd^{2+} connecting with S^{2-} vertically rather than horizontally, as shown in Fig.5[27]. Meanwhile, with the increase of temperature, the stability of complexes decreases. At a relatively high temperature, S^{2-} might be connected the aforementioned complex to form CdS nanostructures along certain direction and the volatile coordinated ligands gradually lost.

In the nanorod cluster, the Cd-complex at the tip of hexagonal crystal ball was first decomposed due to the Coulomb effect. So, the vertical growth speed of the tip was faster than that in the other direction, which led finally to an oriented growth along the axis. In the flowerlike structure, the reduced speed on the surface of smooth micro sphere was the same at any direction. So, the CdS particles suspending in solution conglutinated stochastically to the ball. Under both ethylenediamine template function and surface effect, the CdS nanometer particles were assembled to chain to the surface of microball. With time passing and temperature rising, the joints between the particles were filled with Cd-complex due to the lower stability of joints. Further work is underway to investigate the growth mechanism of self-assembly of flowerlike structure in the final stage. The surface of the petals in the flowerlike structure was very smooth, probably due to Ostwald ripening[28]. Many factors, such as van der Waals force, crystal-face attraction, electrostatic, and hydrogen bond, especially the template, may have various effects on the self-assembly[2,29].

The PL behaviors of CdS nanostructures have been intensively studied[30]. According to previous studies, generally there are two PL emissions of CdS nanostructures, namely band-edge and surface-defect emissions. Due to the quantum confinement effect, the PL peak positions of the band-edge emission of the nanostructures are strongly size-dependent, usually in the wave-

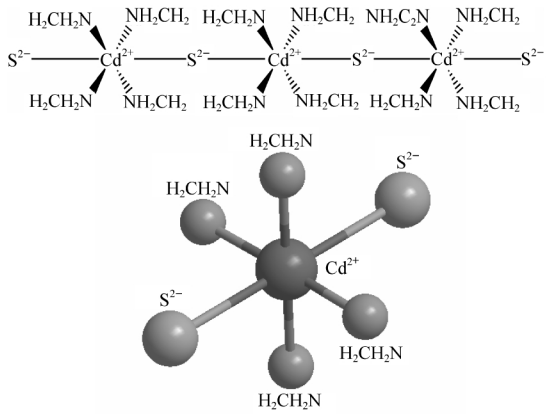

Fig.5 Structure of the Cd-complex[27]

length range of 350−500 nm for CdS. On the other hand, the surface-defect emission is caused by surface states, such as sulphur vacancies and/or sulphur dangling bonds. The PL peak positions of the surface-defect emissions are usually in the wavelength range of 500−700 nm.

Fig.6 shows the PL spectra of CdS samples measured at room temperature at an excitation wavelength of 418 nm. As shown, a blue emission near 430 nm was clearly observed in all the three kinds of CdS samples, but for a slight blue shift in CdS nanostructures with the particle size decreased, which is in agreement with the previous report[31]. Another green emission was observed at 545−565 nm, but the fluorescence intensity of CdS nanorod cluster was significantly weaker than that of commerce CdS products, even than that disappearing in the curve of flowerlike CdS nanostructure. This is attributable to the recombination of an electron trapped in a sulfur vacancy with a hole in the valence band of CdS[32]. The reduction of fluorescence at a long wavelength indicates that the surface-defect of self-assembly CdS nanostructures is much less than that of the commerce CdS product. And the decrease of surface-defect enhances the activity of photocatalysis[33].

The photocatalysis decolorization of methyl orange (MeO) in solution is initiated by the photoexcitation of the semiconductor, followed by the formation of electron-hole pair on the surface of catalyst[34].

$$CdS+h\nu \longrightarrow CdS(e^-+h^+) \quad (4)$$

During the course of the photocatalysis, the CdS catalyst in the MeO resolution destroys not only the MeO conjugated system, but also its molecular structure. When the MeO absorbed on the surface of CdS is excited, it injects an electron (e^-) into the conduction band of CdS. The electron (e^-) can reduce molecular oxygen to superoxide anion and later transform to organic peroxides or hydrogen peroxide. Another reactive intermediate which is responsible for the degradation is hydroxyl radical (·OH). The hydroxyl radical is an extremely strong, non-selective oxidant which leads to the partial or complete mineralization of several organic chemicals. After a series of complicated oxidation reaction, the MeO is decomposed to smaller organics and minerals, like CO_2, H_2O, SO_4^{2-} and so on[35].

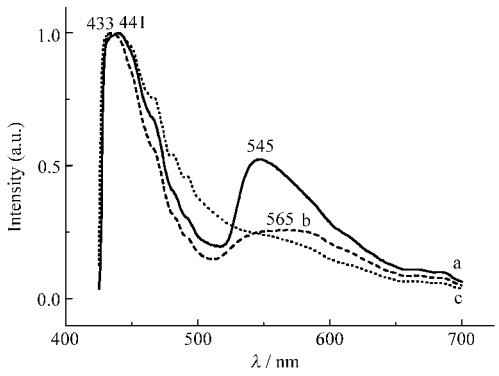

Fig.6 Photoluminescence (PL) spectra of the CdS samples (under 418 nm photoexcitation) at room temperature with the emission spectra normalized to the scale

(a) contrastive CdS powder; (b) CdS nanorod cluster; (c) flowerlike CdS nanostructure

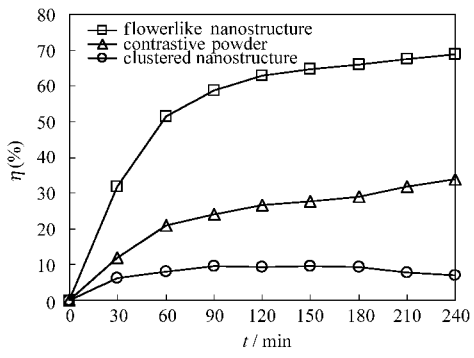

Fig.7 Decolorization efficiency (η) of CdS nanostructures and contrastive CdS powder

Because the direct oxidation of MeO by positive holes (h^+) absorbed on the surface of CdS is considered to be the main oxidation pathway, the specific surface area plays an important role in the speed of photocatalytic process[36]. The BET results show that the specific surface area of flowerlike CdS nanostructure is 20.77 $m^2 \cdot g^{-1}$, the clustered nanostructure is 8.3 $m^2 \cdot g^{-1}$ and the contrastive powder is 10.18 $m^2 \cdot g^{-1}$. Higher specific surface area means that the total active surface area increases at the same catalyst loading, hence availability of more active sites on catalyst surface. In order to prove the effect of the specific surface area, the experiments were performed by comparing in clustered, flowerlike CdS nanostructure and contrastive CdS powder with 0.25 $g \cdot L^{-1}$ catalyst loading for MeO solutions of 40 $mg \cdot L^{-1}$ at natural pH_{start}=6.8. The decolorization efficiency for the three kinds of CdS samples has been depicted in Fig.7. From the figure, it can be seen that the presence of flowerlike nanostructure influences its high photoactivity.

3 Conclusions

In summary, we have used $Cd(NO_3)_2 \cdot 4H_2O$ and $SC(NH_2)_2$ to synthesize nanorod clusters and flowerlike CdS nanostructures *via* an ethylenediamine-mediated solvent thermal process. The reaction mechanism and the self-assembly evolution process were studied with the help of XRD data and SEM images. The PL spectrum showed a blue emission of 433 nm and a green emission centering at nearly 565 nm, which should arise respectively from the excitonic emission and lower surface-defect. The experimental results of BET and photocatalysis confirmed that the flowerlike CdS nanostructure had higher specific surface area and photocatalytic property. The 3D CdS nanostructures may be useful in fabricating some semiconductor devices in the future. The controllable fabrication of the morphology can provide a wide range of compounds with a high specific surface area for the new applications for photocatalysis and so on. We believe that this method can be extended to the nanostructures of other compounds.

References

1 Service, R. F. *Science*, **2005, 309**: 95

2 Whitesides, G. M.; Boncheva, M. *Proc. Natl. Acad. Sci. USA*, **2002, 99**: 4769

3 Park, S.; Lim, J. H.; Chung, S. W.; Mirkin, C. A. *Science*, **2004, 303**: 348

4 Breen, T. L.; Tien, J.; Oliver, S. R. J.; Hadzic, T.; Whitesides, G. M. *Science*, **1999, 284**: 948

5 Gracias, D. H.; Tien, J.; Breen, T. L.; Hsu, C.; Whitesides, G. M. *Science*, **2000, 289**: 1170

6 Cao, A. M.; Hu, J. S.; Liang, H. P.; Wan, L. J. *Angew. Chem. Int. Ed.*, **2005, 44**: 4391

7 Mo, M.; Yu, J. C.; Zhang, L. Z.; Li, S. K. A. *Adv. Mater.*, **2005, 17**: 756

8 Vered, P. Y.; Eugenii, K.; Julian, W.; Itamar, W. *J. Am. Chem. Soc.*, **2003, 125**: 622

9 Guan, G. Q.; Kida, T.; Kusakabe, K.; Kimura, K.; Fang, X. M.; Ma, T. L.; Abe, E.; Yoshida, A. *Chem. Phys. Lett.*, **2004, 385**: 319

10 Lee, J.; Sundar, V. C.; Heine, J. R.; Bawendi, M. G.; Jensen, K. F. *Adv. Mater.*, **2000, 12**: 1102

11 Duan, X. F.; Huang, Y.; Agarwal, R.; Lieber, C. M. *Nature*, **2003, 421**: 241

12 Wu, Y.; Yang, P. *J. Am. Chem. Soc.*, **2001, 123**: 3165

13 Mao, C.; Solis, D. J.; Reiss, B. D.; Kottmann, S. T.; Sweeney, R. Y.; Hayhurst, A.; Georgiou, G.; Iverson, B.; Belcher, A. M. *Science*, **2004, 303**: 213

14 Qian, C.; Kim, F.; Ma, L.; Tsui, F.; Yang, P. D.; Liu, J. *J. Am. Chem. Soc.*, **2004, 126**: 1195

15 Gu, Q.; Cheng, C.; Haynie, D. T. *Nanotechnology*, **2005, 16**: 1358

16 Zhong, H. Z.; Li, Y. C.; Zhou, Y.; Yang, C. H.; Li, Y. Y. *Nanotechnology*, **2006, 17**: 772

17 He, Q. J.; Huang, Z. L.; Liu, Y.; Chen, W.; Xu, T. *Mater. Lett.*, **2007, 61**: 141

18 Zhong, L. S.; Hu, J. S.; Liang, H. P.; Cao, A. M.; Song, W. G.; Wan, L. J. *Adv. Mater.*, **2006, 18**: 2426

19 Fang, X. S.; Ye, C. H.; Zhang, L. D.; Zhang, J. X.; Zhao, J. W.; Yan, P. *Small*, **2005, 1**: 422

20 Wang, Z.; Qian, X. F.; Yin, J.; Zhu, Z. K. *Langmuir*, **2004**, **20**: 3441

21 Muruganandham, M.; Swaminathan, M. *Dyes Pigments*, **2004, 62**: 269

22 Baiocchi, C.; Brussino, C. M.; Pramauro, E.; Prevot, A. B.; Palmisano, L.; Marci, G. *Int. J. Mass Spectrum*, **2002, 214**: 247

23 Fujishima, A.; Honda, K. *Nature*, **1972, 238**: 37

24 Li, Y. D.; Liao, H. W.; Ding, Y.; Qian, Y. T.; Yang, L.; Zhou, G. E. *Chem. Mater.*, **1998, 10**: 2301

25 Wang, Y.; Suna, A.; McHugh, J. *J. Chem. Phys.*, **1990, 92**: 6927

26 Trentler, T. J.; Hickman, K. M.; Goel, S. C.; Viano, A. M.; Gibbons, P. C.; Buhro, W. E. *Science*, **1995, 270**: 1791

27 Nie, Q. L.; Yuan, Q. L.; Xu, Z. D.; Chen, W. X. *Acta Phys. -Chim. Sin.*, **2003**, **19**(12): 1138 [聂秋林, 袁求理, 徐铸德, 陈卫祥. 物理化学学报, **2003**, **19**(12): 1138]

28 Cheng, Y.; Wang, Y. S.; Zheng, Y. H.; Qin, Y. *J. Phys. Chem. B*, **2005, 109**: 11548

29 Colfen, H.; Antonietti, M. *Angew. Chem. Int. Ed.*, **2005, 44**: 5576

30 Lei, Y.; Chim, W. K.; Sun, H. P.; Wilde, G. *Appl. Phys. Lett.*, **2005, 86**: 103106

31 Lubomir, S.; Marc, A. A. *J. Am. Chem. Soc.*, **1990, 112**: 2278

32 Xu, G. Q.; Liu, B.; Xu, S. J.; Chew, C. H.; Chua, S. J.; Gana, L. M. *J. Phys. Chem. Solids*, **2000, 61**: 829

33 Lars, B. R.; Millika, I. *Chemosphere*, **1997, 35**: 585

34 Tang, W. Z.; Huang, C. P. *Water Res.*, **1995, 29**: 745

35 Daneshvar, N.; Salari, D.; Khataee, A. R. *J. Photochem. Photobiol. A*: *Chem.*, **2003, 157**: 111

36 Yang, H. M.; Huang, C. H.; Li, X. W.; Shi, R. R.; Zhang, K. *Mater. Chem. Phys.*, **2005, 90**: 155